A High Order Finite Element Scheme for Pricing Options under Regime Switching Jump Diffusion Processes

Nisha Rambeerich[a] and Athanasios A. Pantelous[b]

[a]*Department of Applied Mathematical Sciences, University of Technology, Mauritius, La Tour Koenig, Pointe-aux-Sables, Mauritius*
[b]*Department of Mathematical Sciences and Institute for Risk and Uncertainty, University of Liverpool, Liverpool, United Kingdom*

Abstract

This paper considers the numerical pricing of European, American and Butterfly options whose asset price dynamics follow the regime switching jump diffusion process. In an incomplete market structure and using the no-arbitrage pricing principle, the option pricing problem under the jump modulated regime switching process is formulated as a set of coupled partial integro-differential equations describing different states of a Markov chain. We develop efficient numerical algorithms to approximate the spatial terms of the option pricing equations using linear and quadratic basis polynomial approximations and solve the resulting initial value problem using exponential time integration. Various numerical examples are given to demonstrate the superiority of our computational scheme with higher level of accuracy and faster convergence compared to existing methods for pricing options under the regime switching model.

Keywords: European and American Option; Regime Switching Model, Finite Element Method, Exponential Time Integration

1. Introduction

1.1. Motivation

In quantitative finance, the seminal works by Black and Scholes [3] and Merton [23] have introduced a performance-free option pricing formula, which does not involve any investor's risk preference or/and subjective views. Ineluctably,

the computational simplicity of the derived compact formula has given it a great popularity in the financial sector. The real economy, however, is occasionally disrupted by structural breaks which generate dramatic transitions in market fundamentals causing the macro-economy and financial markets to switch between distinct recurrent regimes. As a result, there have been several studies conducted by market practitioners and academicians on developing models with the ability to efficiently interpret the economic cycles and the changes in the financial time series data due to the regime shifts.

From the stochastic modelling point of view, exponential Lévy processes of finite and infinite activities have been widely applied to describe the salient distributional and stylized behaviours of skewness and kurtosis in financial asset returns, see for instance [21, 22, 1, 29] and the numerous references therein. Moreover, many research have also successfully been carried out to explain the smile phenomenon by modelling volatility of the underlying asset price by a stochastic process, see for instance [6]. Additionally, originally proposed in [14] for calibrating business phases of expansions and recessions, the regime switching model characterized by a hidden Markov process has become popular in the recent years for modelling the variations in the evolution of asset prices influenced by different macro-economic factors, see also [5]. Indeed, under the Markov switching models, the market parameters depend on states (or regimes) that are determined by an unobserved Markov chain.

Thus, as it will be clearer in the next subsection, the increasing popularity of the regime switching process in option pricing theory is explained mainly due to the inadequacy of the stationary Lévy process to capture cycles of low, moderate and high volatility regimes prevalent in financial markets, which are more appropriately modelled by a Markov process. Further to depicting the jumps in asset prices and the leptokurtic features, a more appealing feature of the regime switching process making it well-known is its ability to model non-linear stylized dynamics of asset returns.

In the next subsection, a brief literature review is presented for the regime switching jump diffusion models, which is the main drive for the numerical pricing of European and American options in the present paper.

1.2. Literature Review - New approach

In the literature of financial mathematics, there are many interesting papers that model option pricing under the regime-switching settings. Starting from Naik [25] back in 1993, for the very first time according to our knowledge, the pricing of the European option under a regime-switching model with two regimes

has been introduced, and this work has been further extended by several other authors.

Under the regime switching model driven by a hidden Markov process, the market is incomplete and thus, a non-unique equivalent martingale measure can be obtained using the Esscher transform technique, see [10]. Among the recent papers on option pricing problems with the underlying asset price dynamics following a Markovian regime switching process, a closed form solution is derived for the perpetual American option in [11] and lattice methods have been employed in [31, 32, 20]. In [5, 4], the authors solve a system of partial differential equations of the governing option pricing problem under the regime switching model, where each partial differential equation represents a regime of the underlying economy. Novel numerical algorithms based on the combination of the θ-scheme and explicit treatment of penalty and regime coupling terms are presented in [17] for the systems of free boundary value problems for pricing American options. In option valuation problems, explicit schemes solving the pricing equations are often subject to stability issues and time-step restrictions. In [15], the authors considered the unconditionally stable Crank-Nicolson time-stepping with fixed point iteration to solve a system of nonlinear algebraic equations, where the regime coupling and penalty terms are treated in an implicit manner. That paper, [15], deals with the pricing of options under the Markov-modulated regime switching process by solving the option pricing problem which is posed as a system of coupled partial differential equations (PDEs).

Several numerical methods have been proposed in the literature to find a fair price of an option under the regime switching jump diffusion model. In [13], the authors use a Fourier Space Time-stepping (FST) procedure for pricing path-dependent options by solving a system of transformed partial integro differential equations (PIDEs) under three states Merton jump diffusion model and achieve second order accurate solutions. A similar approximation technique based on Fourier transform is also proposed in [28]. Bastani et al. [2] price American options by considering a mesh-free approach based on a collocation scheme with radial basis functions combined with the implicit Euler time stepping and the resulting numerical scheme produces super-linear and linear rates of convergence in space and time, respectively. Second order accurate numerical schemes under the regime switching jump diffusion models are derived in [19]. Lee [19] solves the American option linear complementarity problem under regime switching Merton [23] and Kou [18] models by using the finite difference method with three level implicit time stepping coupled with an operator splitting approach to yield second order accuracy with respect to the discrete $\mathcal{L}_2$ norm.

The lattice methods (see [20]) are generally simple to implement under the one-dimensional option pricing framework. However, similar to some finite difference based methods, these schemes are prone to stability problems, yield solutions with low level of accuracy and tend to be computationally demanding for higher dimensional complex path-dependent and multi-asset problems. Furthermore, it is also known that the discontinuity in the payoff function adversely affects the rate of convergence of high order finite difference methods which requires complicated co-ordinate transformations to recover the high order convergence rates often at the cost of increased CPU computational times.

Thus, the numerical schemes proposed in the literature so far achieve at most second order rates of convergence under the regime switching jump diffusion model. The new algorithm developed in the present paper for the numerical pricing of European, American and Butterfly options whose asset price dynamics follow the regime switching jump diffusion process differs from the existing computational schemes. Actually, it considers high order Galerkin finite element in a method of lines approach to initially approximate the spatial terms of the system of partial integro differential equations (PIDEs) and the generated initial value problem is then integrated using the exponential time integration. The finite element method deals with a variational integral formulation of the PIDE and thus, the non - differentiability of the payoff function at the point it forms kink does not hinder the level of accuracy for solving option pricing problems as seen in [26, 27]. As, in [26], to the best of our knowledge, in the present paper, fourth order convergence rates for American options are achieved for the very first time under the quadratic basis functions in the related quantitative finance literature. Finally, we carry out numerous experiments under two and three states regime switching models to show that highly accurate solutions are achieved under both European and American options, where the early exercise feature of the American option is solved by combining the operator splitting mechanism in the exponential time integration. For the data set in [19], our proposed numerical algorithm achieves an accuracy of 10^{-5} using 256 quadratic finite elements and gives an American option value of 13.8313990 whereby in [19], 4096 spatial steps and 3200 time steps are needed to yield the value 13.831394. For European options under three-regime economy, our algorithm yields an error of order 10^{-5} in 13.7330 seconds for 320 quadratic elements and a single time step, in contrast to 180 seconds with 5120 linear elements and 2560 time steps employed for the three-level implicit scheme in [19]. Similarly, under two-regime economy, our proposed numerical algorithm combining ETI scheme and quadratic elements for pricing European options achieves a ratio of error of approximately 16, on refined

meshes, whereas, in [8], the numerical scheme has a ratio of error of 0.5.

This paper is structured in the following manner. In Section 2, we describe the Markov-modulated regime switching jump diffusion framework for option valuation. The variational formulation of the governing pricing equation formulated as a system of PIDEs is considered in Section 3 and time approximation of the resulting initial value problem is discussed in Section 4. The performance of the proposed numerical algorithm is compared with existing discretization methods in terms of level of accuracy, rates of convergence and computational times in Section 5 using various numerical examples. We conclude this study in Section 6.

2. Regime Switching Jump Diffusion Model and Risk-Neutral Option Pricing

We consider a financial market model defined by the filtered probability space $(\Omega, \mathcal{F}, \{\mathcal{F}\}_{t\geq 0}, \mathbf{P})$ consisting of a risk-free and a risky asset with time t prices B_t and S_t, respectively and assume that trading takes place over a finite time horizon $[0, T]$. We let $\{\alpha_t\}_{t\in[0,T]}$ be a continuous-time Markov chain process on $(\Omega, \mathcal{F}, \mathbf{P})$ taking values in a finite state space $\mathcal{H} = \{1, 2, \ldots, H\}$, where each state in $\mathcal{H}$ represents a particular regime.

From Markov chain theory (see for instance, [30]) the generator matrix $\mathbf{Q}$ of the Markov chain $\{\alpha_t\}_{t\in[0,T]}$ is then of order $H \times H$, defined by $\mathbf{Q} = \left(q_{ij}\right)_{H\times H}$, where q_{ij} are transition rates with the property that $q_{ij} \geq 0$, for $i \neq j$ and $\sum_{j=1}^{H} q_{ij} = 0$, for each $i = 1, 2, \ldots H$.

Under the incomplete market framework (see [5], [31]) of the Markov and jumps modulated regime switching process, assuming the absence of arbitrage, we let $\mathbb{Q}$ denote the non-unique equivalent martingale measure derived using the Esscher transform method, see [10]. The risk neutral asset price dynamics paying a continuous dividend yield of δ_{α_t} is then described by the stochastic differential equation given by

$$\frac{dS_t}{S_t} = \left(r_{\alpha_t} - \delta_{\alpha_t} - \lambda_{\alpha_t}\kappa_{\alpha_t}\right) dt + \sigma_{\alpha_t} dW_t + \left(\eta_{\alpha_t} - 1\right) dN_t, \tag{1}$$

where $\{W_t\}_{t\geq 0}$ is a standard Brownian motion, at each economic regime i of α_t, where $r_{\alpha_t} = r_i$ denotes the risk-free rate of interest, $\delta_{\alpha_t} = \delta_i$ is the i^{th}-state dividend yield and $\sigma_{\alpha_t} = \sigma_i$ is the constant volatility. The Poisson process is represented by the stochastic process $\{N_t\}_{t\geq 0}$ with intensity rate being $\lambda_{\alpha_t} = \lambda_i$ at state i and $(\eta_{\alpha_t} - 1) = (\eta_i - 1)$, denotes the impulse function which causes the underlying asset value to jump from S_t to $S_t\eta_i$. The expectation of the impulse function is

then given by $\kappa_{\alpha_t} = \kappa_i$ where $\kappa_i = \mathbb{E}(\eta_i - 1)$. Finally, the stochastic processes $\{W_t\}_{t\geq 0}$, $\{N_t\}_{t\geq 0}$ and $\{\alpha_t\}_{t\in[0,T]}$ in (1) are mutually independent.

We let $V_i(S_t, t)$ denote the time t price of a European option with asset price S_t at regime $\alpha_t = i$. Under the equivalent martingale measure $\mathbb{Q}$ (see [16]), the risk-neutral value of this option with exercise price K and time to maturity T is defined as its expected discounted payoff given by

$$V_i(S_t, t) = \mathbb{E}^{\mathbb{Q}}\left[e^{-r_{\alpha_t}(T-t)}\psi^{(\alpha_t)}(S_T)|\mathcal{F}_t, \alpha_t = i\right],$$

where under each regime $\alpha_t = i$, the payoff for a call option is $\psi^{(i)}(S_T) = \max(S_T - K, 0)$ and for a put option, it is $\psi^{(i)}(S_T) = \max(K - S_T, 0)$. We consider the change of variables $x = \log(S/K)$ and $\tau = T - t$ and we let $U^{(i)}(x, \tau) = V_i(S, \tau)$ denote the value of an option on the transformed space x for regime i.

The price of a European option, $U^{(i)}(x, \tau)$, then solves the constant coefficient forward PIDE given by

$$U^{(i)}_\tau(x, \tau) - \mathcal{L}U^{(i)}(x, \tau) - \sum_{j=1}^{H} q_{ij}U^{(j)}(x, \tau) = 0, \quad \text{for} \quad (x, \tau) \in \mathbb{R} \times [0, T], \tag{2}$$

where

$$\mathcal{L}U^{(i)}(x, \tau) = a_i U^{(i)}_{xx}(x, \tau) + b_i U^{(i)}_x(x, \tau) + c_i U^{(i)}(x, \tau) + \int_{-\infty}^{\infty} U^{(i)}(z, \tau) f(z - x, i)\, dz, \tag{3}$$

with payoff function denoted by $\psi^{(i)}(x)$ and where, under the Merton's model [23], the density function $f(z - x, i)$ with mean μ_i^J and standard deviation σ_i^J is given by

$$f(z - x, i) = \lambda_i \frac{1}{\sqrt{2\pi}\sigma_i^J} \exp\left[-\frac{1}{2}\left(\frac{z - x - \mu_i^J}{\sigma_i^J}\right)^2\right].$$

From equation (3), the coefficients a_i, b_i and c_i are given by

$$a_i = \frac{\sigma_i^2}{2}, \quad b_i = \left(r_i - \delta_i - \frac{\sigma_i^2}{2} - \lambda_i\kappa_i\right) \quad \text{and} \quad c_i = -(r_i + \lambda_i).$$

In order to develop a numerical scheme for the set of PIDEs in (2), we need to define a computational domain Ω_x and hence impose boundary conditions at the truncated ends. These imposed end-conditions depend on the types of options.

For instance, for a European call option, the boundary condition is given by

$$U^{(i)}(x,\tau) = \begin{cases} 0, & x \to -\infty, \\ Ke^{x-\delta_i\tau} - Ke^{-r_i\tau}, & x \to +\infty. \end{cases}$$

Conversely, for a European put option, the option price behaves asymptotically as

$$U^{(i)}(x,\tau) = \begin{cases} Ke^{-r_i\tau} - Ke^{x-\delta_i\tau}, & x \to -\infty, \\ 0, & x \to +\infty. \end{cases}$$

3. Spatial Approximation - The Galerkin Finite Element Method

In order to determine the prices of European options at different regimes, as in [26] (see also relevant references therein) we transform the system of PIDEs (2) using the change of variables $\bar{U}^{(i)}(x,\tau) = U^{(i)}(x,\tau) - \psi^{(i)}(x)$ with $\bar{U}$ being the excess option premium over the payoff function and solve $\bar{U}$ for $i = 1, 2, \ldots, H$ in the system of PIDEs given below

$$\bar{U}^{(i)}_\tau(x,\tau) - \mathcal{L}\bar{U}^{(i)}(x,\tau) - \sum_{j=1}^{H} q_{ij}\bar{U}^{(j)}(x,\tau) = \mathcal{G}\psi^{(i)}(x) + \sum_{j=1}^{H} q_{ij}\psi^{(j)}(x), \qquad (4)$$

where

$$\mathcal{G}\psi^{(i)}(x) = a_i\psi^{(i)}_{xx}(x) + b_i\psi^{(i)}_x(x) + c_i\psi^{(i)}(x) + \int_{-\infty}^{\infty} \psi^{(i)}(z) f(z-x,i)\, dz, \qquad (5)$$

for $(x,\tau) \in \mathbb{R} \times [0,T]$. On the computational domain, the transformed PIDE (4) is then solved subject to homogeneous Dirichlet boundary conditions given by

$$\lim_{|x|\to\infty} \bar{U}^{(i)}(x,\tau) = 0, \qquad (6)$$

and initial condition of $\bar{U}^{(i)}(x,0) = 0$.

Under Merton's model [23], the explicit form of the right-hand-side of equation (5) for a European put option becomes

$$\begin{aligned} \mathcal{G}\psi^{(i)}(x) =& \frac{1}{2}\sigma_i^2 K\delta_{x=0} + \left[\lambda_i(1+\kappa_i) + \delta_i\right] Ke^x \mathbf{1}_{x\le 0} - (r_i+\lambda_i)K\mathbf{1}_{x\le 0} + \lambda_i K\mathcal{N}\left(\frac{-x-\mu_i^J}{\sigma_i^J}\right) \\ & - \lambda_i Ke^{x+\mu_i^J+(\sigma_i^J)^2/2}\mathcal{N}\left(\frac{-x-\mu_i^J-(\sigma_i^J)^2}{\sigma_i^J}\right) + \sum_{j=1}^{H} q_{ij}(K-Ke^x)\mathbf{1}_{x\le 0}, \qquad (7) \end{aligned}$$

for $i = 1, 2, \ldots, H$ and for a European call option, we get

$$\mathcal{G}\psi^{(i)}(x) = \frac{1}{2}\sigma_i^2 K\delta_{x=0} - \left[\lambda_i(1+\kappa_i) + \delta_i\right] Ke^x \mathbf{1}_{x\geq 0} + (r_i + \lambda_i)K\mathbf{1}_{x\geq 0} - \lambda_i K\mathcal{N}\left(\frac{x+\mu_i^J}{\sigma_i^J}\right)$$
$$+ \lambda_i K e^{x+\mu_i^J+(\sigma_i^J)^2/2}\mathcal{N}\left(\frac{x+\mu_i^J+(\sigma_i^J)^2}{\sigma_i^J}\right) + \sum_{j=1}^{H} q_{ij}(Ke^x - K)\mathbf{1}_{x\geq 0}, \qquad (8)$$

where $\mathcal{N}(z)$ denotes the cumulative normal distribution.

3.1. Weak Variational Formulation

In order to carry a spatial discretization of the PIDE (4), we must localize the spatial domain from $\mathbb{R}$ to $\Omega_x = (x_{\min}, x_{\max})$. We sub-divide the interval Ω_x into M finite elements, denoting by Ω_x^e a single finite element and construct a finite element mesh with equidistant nodes, x_i, and define a space step $h = (x_{\max} - x_{\min})/M$. The next Theorem is giving the weak variational form of equation (4) under linear and quadratic finite elements, which is one of the main results of the present paper.

Theorem 3.1. *A weak variational form of (4) is given by*

$$\sum_{e=1}^{M}\int_{\Omega_x^e}\sum_{l=1}^{n}\phi_k^e\phi_l^e u_l'^{e,i}(\tau)dx + \sum_{e=1}^{M}\int_{\Omega_x^e}\sum_{l=1}^{n}\left[a_i\frac{\partial\phi_k^e}{\partial x}\frac{\partial\phi_l^e}{\partial x} - b_i\phi_k^e\frac{\partial\phi_l^e}{\partial x} - c_i\phi_k^e\phi_l^e\right]u_l^{e,i}(\tau)dx$$
$$- \sum_{e=1}^{M}\int_{\Omega_x^e}\sum_{l=1}^{n}\sum_{j=1}^{H} q_{ij}\phi_k^e\phi_l^e u_l^{e,j}(\tau)dx - \sum_{e=1}^{M}\int_{\Omega_x^e}\phi_k^e\left(\sum_{e=1}^{M}\int_{\Omega_x^e}\sum_{l=1}^{n}\phi_l^e u_l^{e,i}(\tau)f(z-x,i)\,dz\right)dx$$
$$= \sum_{e=1}^{M}\int_{\Omega_x^e}\phi_k^e\left[\mathcal{G}\psi^{(i)}(x) + \sum_{j=1}^{H} q_{ij}\psi^{(j)}(x)\right]dx, \quad k = 1, 2, \ldots, n, \qquad (9)$$

where for linear finite elements with $\left\{x_i^e, x_{i+1}^e\right\} \in \Omega_x^e$,

$$\begin{aligned}\phi_1^e(x) &= \frac{x_{i+1}^e - x}{x_{i+1}^e - x_i^e},\\ \phi_2^e(x) &= \frac{x - x_i^e}{x_{i+1}^e - x_i^e},\end{aligned} \qquad (10)$$

and for quadratic finite elements with $\left\{x_i^e,\, x_{i+1}^e,\, x_{i+2}^e\right\} \in \Omega_x^e$,

$$\begin{aligned}
\phi_1^e(x) &= \frac{(x - x_{i+1}^e)(x - x_{i+2}^e)}{(x_i^e - x_{i+1}^e)(x_i^e - x_{i+2}^e)}, \\
\phi_2^e(x) &= \frac{(x - x_i^e)(x - x_{i+2}^e)}{(x_{i+1}^e - x_i^e)(x_{i+1}^e - x_{i+2}^e)}, \\
\phi_3^e(x) &= \frac{(x - x_i^e)(x - x_{i+1}^e)}{(x_{i+2} - x_i^e)(x_{i+2}^e - x_{i+1}^e)}.
\end{aligned} \tag{11}$$

Finally, a_i, b_i, c_i, $\mathcal{G}$ *and* $f(z - x, i)$ *have been already defined before (see previous sections).*

Proof. Let us first multiply the system (4) by a weight function $\vartheta(x) \in L_2(\Omega_x)$ with the property that $\vartheta(x)$ vanishes on the end boundaries $\partial\Omega_x$ and then, integrate the result over the domain Ω_x to obtain

$$\begin{aligned}
&\int_{\Omega_x} \vartheta \bar{U}_\tau^{(i)} + a_i \vartheta_x \bar{U}_x^{(i)} - \vartheta \left(b_i \bar{U}_x^{(i)} + c_i \bar{U}^{(i)} \right) dx - \int_{\Omega_x} \vartheta \left(\sum_{j=1}^{H} q_{ij} \bar{U}^{(j)} \right) dx \\
&- \int_{\Omega_x} \vartheta \left(\int_{\mathbb{R}} \bar{U}^{(i)}(z, \tau) f(z - x, i)\, dz \right) dx \\
&= \int_{\Omega_x} \vartheta \mathcal{G} \psi^{(i)}(x)\, dx + \int_{\Omega_x} \vartheta \left(\sum_{j=1}^{H} q_{ij} \psi^{(j)}(x) \right) dx,
\end{aligned} \tag{12}$$

for $i = 1, 2, \ldots, H$ with initial condition given by

$$\int_{\Omega_x} \vartheta \bar{U}^{(i)}(x, 0)\, dx = 0.$$

The finite element approximation employed in the following is based on an element-wise assembly procedure. Therefore, the weak variational form (12) is re-written in terms of a sum of integrals over a finite element of sub-domain Ω_x^e as given below,

$$\begin{aligned}
&\sum_{e=1}^{M} \left[\int_{\Omega_x^e} \vartheta \bar{U}_\tau^{(i)} + a_i \vartheta_x \bar{U}_x^{(i)} - \vartheta \left(b_i \bar{U}_x^{(i)} + c_i \bar{U}^{(i)} \right) dx - \int_{\Omega_x^e} \vartheta \left(\sum_{j=1}^{H} q_{ij} \bar{U}^{(j)} \right) dx \right. \\
&\left. - \int_{\Omega_x^e} \vartheta \left(\int_{\mathbb{R}} \bar{U}^{(i)}(z, \tau) f(z - x, i)\, dz \right) dx \right] \\
&= \sum_{e=1}^{M} \int_{\Omega_x^e} \vartheta \mathcal{G} \psi^{(i)}(x)\, dx + \sum_{e=1}^{M} \int_{\Omega_x^e} \vartheta \left(\sum_{j=1}^{H} q_{ij} \psi^{(j)}(x) \right) dx
\end{aligned} \tag{13}$$

with initial condition given by

$$\sum_{e=1}^{M} \int_{\Omega_x^e} \vartheta \bar{U}^{(i)}(x,\, 0)\, dx = 0.$$

Over each finite element Ω_x^e, we let $\bar{U}^{(i)}$ in (13) be defined by a linear combination of Lagrangian basis functions $\phi_l^e(x)$, where for linear and for quadratic finite elements, see (10) and (11), respectively. Thus,

$$\bar{U}^{(i)}(x,\, \tau) = \sum_{l=1}^{n} \phi_l^e(x) u_l^{e,i}(\tau), \tag{14}$$

where the $u_l^{e,i}(\tau)$ are unknowns that must be determined and n denotes the number of nodes. Therefore, substituting (14) and letting the weight function equal to the basis function under the Galerkin method, we obtain the following representation for the weak form(13) with no non-local jump integral

$$\begin{aligned}
&\sum_{e=1}^{M} \int_{\Omega_x^e} \sum_{l=1}^{n} \phi_k^e \phi_l^e u_l'^{e,i}(\tau) dx + \sum_{e=1}^{M} \int_{\Omega_x^e} \sum_{l=1}^{n} \left[a_i \frac{\partial \phi_k^e}{\partial x} \frac{\partial \phi_l^e}{\partial x} - b_i \phi_k^e \frac{\partial \phi_l^e}{\partial x} - c_i \phi_k^e \phi_l^e \right] u_l^{e,i}(\tau) dx \\
&- \sum_{e=1}^{M} \int_{\Omega_x^e} \sum_{l=1}^{n} \sum_{j=1}^{H} q_{ij} \phi_k^e \phi_l^e u_l^{e,j}(\tau) dx,
\end{aligned} \tag{15}$$

for $k = 1, 2, \ldots, n$. Finally, the Galerkin approximation for the jump integral term with regimes i is given by

$$\begin{aligned}
&\int_{\Omega_x} \vartheta \left(\int_{\mathbb{R}} \bar{U}^{(i)}(z, \tau) f(z - x, i)\, dz \right) dx \\
&\qquad = \sum_{e=1}^{M} \int_{\Omega_x^e} \phi_k^e \left(\sum_{e=1}^{M} \int_{\Omega_x^e} \sum_{l=1}^{n} \phi_l^e u_l^{e,i}(\tau) f(z - x, i)\, dz \right) dx.
\end{aligned} \tag{16}$$

□

Remark 1. The representation on the right-hand-side of the jump integral term, (16), for the linear elements is approximated by

$$\sum_{e=1}^{M} \int_{\Omega_x^e} \begin{pmatrix} \phi_1^e \\ \phi_2^e \end{pmatrix} \mathcal{J} dx,$$

where

$$\mathcal{J} = \frac{h}{2}\left(u_0^{(i)}(\tau) f(x_0 - x, i) + 2\sum_{l=1}^{M-1} u_l^{(i)}(\tau) f(x_l - x, i) + u_M^{(i)}(\tau) f(x_M - x, i) \right),$$

and similarly, for the quadratic finite elements is approximated by

$$\sum_{e=1}^{M} \int_{\Omega_x^e} \begin{pmatrix} \phi_1^e \\ \phi_2^e \\ \phi_3^e \end{pmatrix} \mathcal{J}\, dx,$$

where

$$\mathcal{J} = \frac{h}{6}\sum_{l=1}^{M} \left[f(x_{2l-2} - x, i) u_{2l-2}^{(i)}(\tau) + 4 f(x_{2l-1} - x, i) u_{2l-1}^{(i)}(\tau) + f(x_{2l} - x, i) u_{2l}^{(i)}(\tau) \right].$$

3.2. The Semi-Discrete System

Under the regime switching model, the spatial approximation using finite element method explained in Subsection 3.1 and by Theorem 3.1 leads to a set of initial value problems that must be solved using appropriate time stepping methods. We thus obtain a system of ordinary differential equations given by

$$\mathbf{M}\mathbf{u}'(\tau) + (\mathbf{S} - \mathbf{J})\mathbf{u}(\tau) = \mathbf{f}, \tag{17}$$

with mass matrix $\mathbf{M}$, stiffness matrix $\mathbf{S}$, jump integral matrix $\mathbf{J}$ and load vector $\mathbf{f}$. Under each regime i, the mass matrix, denoted by $\mathbf{M}_x$, the stiffness matrix, denoted by $\mathbf{S}_x$ and jump integral matrix, denoted by $\mathbf{J}_x$ are derived from (15) and (16). The load vector $\mathbf{f}$ is derived from the right-hand-side of (13). The matrices and load vector result after adjusting for the homogeneous Dirichlet boundary conditions (6).

The mass matrix $\mathbf{M}$ is derived using the Kronecker product, $\otimes$, of the identity matrix $\mathbf{I}$ of order $H \times H$ and mass matrix $\mathbf{M}_x$ and is given by

$$\mathbf{M} = \mathbf{I} \otimes \mathbf{M}_x.$$

For linear finite elements, the matrix $\mathbf{M}_x$ is found by assembling element matrices

$$\frac{h}{6}\begin{pmatrix} 2 & 1 \\ 1 & 2 \end{pmatrix},$$

over a fixed number of linear finite elements and imposing the homogeneous boundary conditions on the resulting global matrix. In a similar manner, for quadratic basis functions, $\mathbf{M}_x$ is generated by the assembly of 3×3 matrices

$$\frac{h}{30}\begin{pmatrix} 4 & 2 & -1 \\ 2 & 16 & 2 \\ -1 & 2 & 4 \end{pmatrix},$$

over the number of quadratic finite elements and then adjusting for the boundary conditions on the resulting global matrix.

For the stiffness matrix $\mathbf{S}$, we have the following representation

$$\mathbf{S} = \mathbf{diag}\,(a_1,\, a_2,\, \ldots, a_H) \otimes \mathbf{D} - \mathbf{diag}\,(b_1,\, b_2,\, \ldots, b_H) \otimes \mathbf{A} \\ - \mathbf{diag}\,(c_1,\, c_2,\, \ldots, c_H) \otimes \mathbf{M} - \mathbf{Q} \otimes \mathbf{M}, \quad (18)$$

where matrix $\mathbf{D}$ is the matrix corresponding to the diffusion term generated from the inner product

$$\left(\phi_k'^e, \phi_l'^e\right)_{L^2(\Omega_x)} = \sum_{e=1}^{M} \int_{\Omega_x^e} \frac{\partial \phi_k^e}{\partial x} \frac{\partial \phi_l^e}{\partial x} dx,$$

and $\mathbf{A}$ is the matrix derived using the inner product representation

$$\left(\phi_k^e, \phi_l'^e\right)_{L^2(\Omega_x)} = \sum_{e=1}^{M} \int_{\Omega_x^e} \phi_k^e \frac{\partial \phi_l^e}{\partial x} dx.$$

The jump integral matrix $\mathbf{J}$ is constructed using the **blkdiag** function in Matlab, by assembling the jump matrices under distinct regimes.

4. Exponential Time Integration (ETI)

In this section, we apply exponential time integration to solve the initial value problem (17) in the interval $[0,\, T]$. For an European option, the system (17) is solved in a single time step and the solution is given by

$$\mathbf{u}(T) = \mathbf{A}^{-1}\left(e^{\mathbf{A}T} - \mathbf{I}\right)\mathbf{b}, \quad (19)$$

where $\mathbf{I}$ is the identity matrix of same size as matrix $\mathbf{A}$, and matrix $\mathbf{A}$ and vector $\mathbf{b}$ in (19) are given by

$$\mathbf{A} = -\mathbf{M}^{-1}(\mathbf{S} - \mathbf{J}), \quad \mathbf{b} = \mathbf{M}^{-1}\mathbf{f},$$

respectively. We note that the solution for European options using the exponential time integration technique consists of evaluating the form $\mathbf{A}^{-1}\left(e^{\mathbf{A}T}-\mathbf{I}\right)$. The evaluation of the matrix $\mathbf{A}$ and the vector $\mathbf{b}$ can be efficiently carried out, mainly due to the fact that matrix $\mathbf{M}$ is sparse. Several methods for computing $\mathbf{A}^{-1}\left(e^{\mathbf{A}T}-\mathbf{I}\right)$ have been proposed in the literature among which [24] considers a matrix decomposition mechanism and is the cheapest in terms of computational time with a level of accuracy comparable to the explicit evaluation of the formula $\mathbf{A}^{-1}\left(e^{\mathbf{A}T}-\mathbf{I}\right)$. Our algorithm implements this term explicitly using Matlab's expm and inv functions. In order to obtain the option price at time T, we add the payoff $\psi^i(x)$, for all $i = 1, 2, \ldots, H$ to $\mathbf{u}(T)$ obtained in (19).

4.1. American options

The American option pricing problem is formulated as a linear complimentarily problem, given by

$$
\begin{aligned}
&U_\tau^{(i)}(x,\tau) - \mathcal{L}U^{(i)}(x,\tau) - \sum_{j=1}^{H} q_{ij}U^{(j)}(x,\tau) \geq 0, \quad (x,\,\tau) \in \mathbb{R}\times(0,\,T],\\
&U^{(i)}(x,\tau) - U^{(i)}(x,0) \geq 0, \quad U^{(i)}(x,0) = \psi^{(i)}(x),\\
&\left(U_\tau^{(i)}(x,\tau) - \mathcal{L}U^{(i)}(x,\tau) - \sum_{j=1}^{H} q_{ij}U^{(j)}(x,\tau)\right)\left(U^{(i)}(x,\tau) - U^{(i)}(x,0)\right) = 0. \quad (20)
\end{aligned}
$$

The operator splitting technique [12] applied to (20) leads to solving a linear PIDE problem of the form given by

$$
U_\tau^{(i)}(x,\tau) - \mathcal{L}U^{(i)}(x,\tau) - \sum_{j=1}^{H} q_{ij}U^{(j)}(x,\tau) = \Lambda^{(i)}(\tau), \tag{21}
$$

where $\Lambda^{(i)}(\tau)$ is a penalty term satisfying $\Lambda^{(i)}(\tau) \geq 0$. In order to satisfy the requirement that the value of the American option is at least the payoff, additional constraints need to be enforced as given below:

$$
\begin{aligned}
&\left(U^{(i)}(x,\tau) - U^{(i)}(x,0\right)\cdot\Lambda^{(i)}(\tau) = 0,\\
&U^{(i)}(x,\tau) \geq \psi^{(i)}(x), \quad (x,\,\tau) \in \mathbb{R}\times(0,\,T].
\end{aligned}
$$

Since we solve for an excess to payoff value, the numerical scheme for pricing an American option using the method of finite elements, exponential time integration and operator splitting technique is given by

$$
\mathbf{M}\mathbf{u}'(\tau) + (\mathbf{S}-\mathbf{J})\mathbf{u}(\tau) = \mathbf{f} + \mathbf{f_1}\cdot\Lambda(\tau). \tag{22}
$$

In order to derive the vector $\mathbf{f_1}$, we first consider the finite element approximation given by

$$\mathcal{H} = \sum_{e=1}^{M} \int_{\Omega_x^e} \vartheta \, dx. \tag{23}$$

We then perform a Kronecker product using the resulting vector $\mathbf{h}$, obtained from (23), in the following way

$$\mathbf{f_1} = \begin{pmatrix} 1 \\ \vdots \\ 1 \end{pmatrix}_{H \times 1} \otimes \mathbf{h}.$$

Thus, $\mathbf{f_1} \cdot \Lambda(\tau)$ is the vector obtained by componentwise multiplications of the elements in $\mathbf{f_1}$ and $\Lambda(\tau)$.

To solve the system (22), we rewrite it as

$$\mathbf{u}'(\tau) = \mathbf{A}\mathbf{u}(\tau) + \mathbf{M}^{-1} \left(\mathbf{f} + \mathbf{f_1} \cdot \Lambda(\tau) \right),$$

with initial condition being $\mathbf{u}(0) = \mathbf{0}$.

We then define a uniform time mesh $\tau^n = nk$, for $n = 0, 1, 2, \ldots, N$ with constant time step $k = T/N$. At time τ^{n+1}, the solution is given by

$$\bar{\mathbf{u}}\left(\tau^{n+1}\right) = e^{\mathbf{A}k}\mathbf{u}\left(\tau^n\right) + \mathbf{A}^{-1}\left(e^{\mathbf{A}k} - \mathbf{I}\right)\mathbf{b}\left(\tau^n\right),$$

where $\mathbf{b}\left(\tau^n\right) = \mathbf{M}^{-1}\left(\mathbf{f} + \mathbf{f_1} \cdot \Lambda(\tau^n)\right)$. The vector $\mathbf{u}\left(\tau^{n+1}\right)$ is then obtained by enforcing the constraints

$$\mathbf{u}\left(\tau^{n+1}\right) = \max\left(\mathbf{0},\, \bar{\mathbf{u}}\left(\tau^{n+1}\right) - k\Lambda(\tau^n)\right),$$

and

$$\Lambda(\tau^{n+1}) = \Lambda(\tau^n) + \frac{1}{k}\left(\mathbf{u}\left(\tau^{n+1}\right) - \bar{\mathbf{u}}\left(\tau^{n+1}\right)\right),$$

respectively, where $\Lambda(\tau^0) = \mathbf{0}$. To find the American option value, we add the payoff function to the solution vector $\mathbf{u}\left(\tau^{N+1}\right)$.

5. Numerical Experiments

In this section, we demonstrate the performance of the proposed computational scheme for pricing European and American options under Merton's jump

diffusion model for two-state and three-state regimes. We also consider the pricing of Butterfly call option under the three-state regime switching model. All codes are run in Matlab® R2010a with 8.00GB RAM and 2.90 Ghz processor. In the sequel, 'Error' refers to the difference between successive numerical solutions following mesh refinements, given by

$$\text{Error} = |\text{Price}_M - \text{Price}_{2M}|,$$

and 'Ratio' denotes the ratio of errors.

5.1. Two-State Regimes

The first test example prices a European put option using linear and quadratic finite elements and the ETI scheme. The results are reported in Table 1 at the points where the strike price K equals the spot value $S = 40$, and the data set in [8] is used, where the rate of interest and the dividend yield under both regimes are $r_i = 0.08$ and $\delta_i = 0$, respectively and the jump parameters for $i = 1, 2$ are

$$\mu_i^J = -0.025, \quad \sigma_i^J = \sqrt{0.05}, \quad \lambda_i = 5,$$

with time to maturity $T = 1$, strike price $K = 40$ and the generator matrix $\mathbf{Q}$ given by

$$\begin{pmatrix} -0.5 & 0.5 \\ 0.5 & -0.5 \end{pmatrix}.$$

[Insert TABLE 1 about here]

The computational domains under Regimes 1 and 2 are set at $\Omega_x = [-3, 3]$ and $\Omega_x = [-2.5, 2.5]$, respectively. The prices for the European option with volatilities $\sigma_1 = 0.3$ and $\sigma_2 = 0.1$ are computed such that the number of quadratic elements is half the number of linear elements. Under linear elements, second order convergence rates are achieved for both $\sigma_1 = 0.3$ and $\sigma_2 = 0.1$, indicated by a ratio of errors of 4. Under the quadratic elements, we find that ratios of errors of approximately 16 are achieved as the mesh sizes are refined, thus indicating very high level of accuracy. In [28] and [8], the option prices obtained for $\sigma_1 = 0.3$ are 7.0372 and 7.0369 respectively, and similarly for $\sigma_2 = 0.1$, they are given by 6.3165 and 6.3162, respectively. To our knowledge, this paper is the first to achieve such high rates of convergence with ratio of errors of approximately 16 under regime switching jump diffusion models. The ETI scheme is an efficient time integration method for option valuation as it solves for the European option value in a single

time step and no difficulty is faced when evaluating the matrix exponential for reasons outlined in [26] and [27]. A comparison of the numerical solutions listed in Table 1 shows that few quadratic Lagrange basis functions lead to highly accurate solutions. We find that under Regime 1, 80 quadratic elements result in an accuracy of 10^{-3} whereas 320 linear elements are required to reach the same level of accuracy. A similar observation is made for Regime 2 solutions where the accuracy 10^{-4} is achieved using 1280 linear elements compared to 160 quadratic basis functions. In addition, the option value 7.0369172 is achieved using 640 quadratic finite elements producing an accuracy of 10^{-7} computed in only a single time step, whereas in [8], the solution is 7.0369 generated using $N = 2000$ time steps. Similarly, we note that 640 quadratic finite elements lead to the option value 6.3162802 with a level of accuracy of 10^{-6}, whereas [8] uses $N = 2000$ time-steps to obtain 6.3177.

[Insert TABLE 2 about here]

Table 2 lists the prices of an American put option calculated using the data set in [8], at the point where strike price $K = 40$ equals the spot value, S and with time to maturity, $T = 1$. We observe that the linear elements achieve second order rates of convergence and quadratic basis functions yield very high level of accuracy, for both the high and the low volatility regimes. Comparing our solutions to those obtained in [8], we find that the numerical scheme in [8] for pricing the American put option under the high volatility regime $\sigma_1 = 0.3$ and the low volatility regime $\sigma_2 = 0.1$ produces a ratio of error which is near to 0.5. In addition, we find that 320 quadratic elements give a level of accuracy of 10^{-6} and 10^{-5} with American option price 7.3814864 and 6.6292392, respectively, using 640 time intervals whereas, in [8], larger time intervals must be considered to attain the solutions 7.3810 and 6.6304.

[Insert TABLE 3 about here]

[Insert TABLE 4 about here]

5.2. Three-State Regime

The solutions in both Table 3 and Table 4 are computed using the data in [19], which for a three state economy under regime-switching Merton model are as follows:

$$\sigma_i = 0.15, \quad r_i = 0.05, \quad \delta_i = 0, \quad \mu_i^J = -0.5, \quad \sigma_i^J = 0.45,$$

with jump intensities λ_i and generator matrix $\mathbf{Q}$ given by

$$\mathbf{Q} = \begin{pmatrix} -0.8 & 0.6 & 0.2 \\ 0.2 & -1.0 & 0.8 \\ 0.1 & 0.3 & -0.4 \end{pmatrix}, \quad \text{and} \quad \lambda = \begin{pmatrix} 0.3 \\ 0.5 \\ 0.7 \end{pmatrix}.$$

The values of the jump intensities and the generator matrix are chosen as in the papers by [2, 13] and [19]. The exercise price is $K = 100$ and the time to maturity is $T = 1$. The solutions reported in both Tables 3 and 4 are at the point where the strike price, K equals the spot value, $S = 100$. Table 3 lists the prices for European put options at jump intensities $\lambda_1 = 0.3$, $\lambda_2 = 0.5$ and $\lambda_3 = 0.7$, respectively. The computational domain for all the three regimes is $\Omega_x = [-4.6, 4.6]$. The linear elements yield quadratic rates of convergence under each regime for $\lambda_1 = 0.3$, $\lambda_2 = 0.5$ and $\lambda_3 = 0.7$, respectively. On the other hand, we find that quadratic finite elements lead to ratios of errors of approximately 16 for all the three states of the economy. We also note that the price of the European put option at the first state of the economy under the regime-switching Merton model at $S = K = 100$ in [19] is 10.545878 achieved using 4096 and 3200 spatial and time steps, respectively. In Table 3, we obtain 10.5458970 using 640 quadratic finite elements and 10.5450898, using 1280 linear finite elements and single time step. The efficiency of the combination of quadratic basis functions and ETI scheme is clearly demonstrated by the numerical solutions reported in Table 3 for all three regimes, where 160 quadratic elements result in an error of order 10^{-3} and 10^{-4} whereas, 1280 linear elements are required to achieve the same level of accuracy.

Next, we compute the American put option prices for the three states of the economy, with $\lambda_1 = 0.3$, $\lambda_2 = 0.5$ and $\lambda_3 = 0.7$, see Table 4, where the domain of computation is set to $\Omega_x = [-3.5, 3.5]$.

Similar to previous numerical experiments considered in the subsections above, we achieve better solutions in terms of accuracy for quadratic elements. For instance, only 256 quadratic elements and 512 time steps are required to achieve a solution of 13.8313990 for the second state of the economy. In [19], the solution obtained for the same set of parameters is 13.831394 using 4096 spatial steps and 3200 time steps. Furthermore, In Table 4, we find that quadratic elements yield an accuracy of 10^{-5} using 256 elements whereas 4096 spatial steps are required to attain the same level of accuracy in [19].

[Insert TABLE 5 about here]

The following numerical example concerns the pricing of a butterfly call option using the combination of ETI and linear and quadratic basis functions with the

3×3 generator matrix $\mathbf{Q}$. We show through the results displayed in Table 5 that the proposed numerical algorithm is very efficient for pricing options other than the vanilla type options.

[Insert FIGURE 1 about here]

Figure 1 illustrates the solution for the European Butterfly call option under Regimes 1, 2 and 3 using the ETI scheme combined with 320 quadratic elements for the data sets in Table 5.

5.3. Comparison of Proposed Scheme with Other Time Stepping Methods in Three Regime Economy

This subsection considers the numerical comparison of the ETI scheme with quadratic elements and the three-time levels method described in [19] for pricing European put. For the purpose of the comparison, we have applied the three-time levels method to the systems of initial value problem obtained using the linear finite element approximation technique, where solutions at the initial time steps are obtained using the first order implicit-explicit scheme in [7]. The data set used in the following numerical test is $\sigma_1 = 0.15$, $r_1 = 0.03$, $\delta_1 = 0$, $\mu_1^J = 0$, $\sigma_1^J = 0.3$,$\lambda_1 = 0.3$ and generator matrix

$$\mathbf{Q} = \begin{pmatrix} -0.8 & 0.6 & 0.2 \\ 0.2 & -1.0 & 0.8 \\ 0.1 & 0.3 & -0.4 \end{pmatrix}.$$

The time to maturity is $T = 0.5$ years and strike price $K = 100$. The solutions are listed in Table 6 at spot prices 90, 100 and 110, with computational domain $\Omega_x = [-3.2, 3.2]$ and they correspond to Regime 1 of the economy. CPU refers to the computational speed of the numerical scheme at given number of nodes.

[Insert TABLE 6 about here]

We find that the quadratic elements are very efficient leading to high level of accuracies and combined with the ETI scheme yields the solution in a single time-step for European options. Under Merton jump diffusion model, the normally distributed jump sizes helps to achieve high convergence rates with solutions of high level of accuracies when the finite element method with quadratic basis polynomials is employed. However, as mentioned in [9], under Kou's model, the discontinuity at zero in the double-exponentially distributed density function in the

jump integral term is a major drawback for numerical schemes and hence leads to approximately linear rates of convergence and low accuracy level-solutions.

At all spot prices $S = 90$, 100, 110, an error of order 10^{-6} is achieved using 640 quadratic elements. We also observe that an error of order 10^{-4} is achieved using only 160 quadratic elements in 1.5 seconds and one time step, whereas the three-level method requires 2560 linear elements with 1280 time steps and 25 seconds to reach the same level of accuracy. Refining further the spatial and temporal mesh sizes to 5120 and 2560, respectively costs 180 seconds to obtain the solution 9.7088972, 4.1776186, and 1.6333618, at spot prices 90, 100 and 110, respectively producing an error of order 10^{-5}. The latter is achieved in a mere 13.7330 seconds with our proposed numerical scheme combining quadratic elements and ETI.

[Insert TABLE 7 about here]

Table 7 contains the numerical solutions for American put options for the three regimes for varying volatilities, rates of interest and jump parameters and generator matrix

$$\mathbf{Q} = \begin{pmatrix} -0.8 & 0.6 & 0.2 \\ 0.2 & -1.0 & 0.8 \\ 0.1 & 0.3 & -0.4 \end{pmatrix}.$$

The solutions are computed using the Crank-Nicolson time-stepping scheme, the three-level implicit method and ETI scheme with linear and quadratic elements whereby the early exercise feature of the American option is catered for by the application of the operator splitting mechanism. For the Crank-Nicolson time stepping scheme and the three level implicit scheme, we use linear finite elements for the spatial approximation. We illustrate the performance of the listed time integration methods with test examples such that a distinct data set is considered for each regime. All the results displayed in Table 7 are at the point where strike price, K, equals spot value, that is at $K = 100$.

Under Regime 1, we use volatility $\sigma_1 = 0.13$, rate of interest $r_1 = 0.04$ and jump parameters $\mu_1^J = -0.2$, $\sigma_1^J = 0.25$ and $\lambda_1 = 2$. The solutions are computed within the bounded domain $\Omega_x = [-3.5, 3.5]$ and time to maturity is given by $T = 0.5$ years. Under the Crank-Nicolson scheme, the jump integral term is treated explicitly using the fixed point iteration method. The fast Fourier transform technique is applied for evaluating the matrix-vector multiplication corresponding to the jump integral term, under both the Crank-Nicolson and the three-level methods. Table 7 shows that the Crank-Nicolson scheme, the three-level scheme and the ETI scheme combined with linear basis functions achieve an error of order 10^{-3} using

1280 linear finite elements and 640 time steps. However, the quadratic based ETI scheme produces the same accuracy using 160 elements.

We make similar observations for American option prices computed under Regime 2 and 3. For Regime 2, the data set used are $\sigma_2 = 0.2$, $r_2 = 0.02$, $\mu_2^J = 0$, $\sigma_2^J = 0.3$ and $\lambda_2 = 0.8$ and time to expiry is 0.5 years with strike price $K = 100$ and $\Omega_x = [-3.6, 3.6]$. Under Regime 3, we use the parameters $\sigma_3 = 0.15$, $r_3 = 0.07$, $\mu_3^J = 0.1$, $\sigma_3^J = 0.35$ and $\lambda_3 = 1$ and time to expiry is 0.5 years with strike price $K = 100$ and $\Omega_x = [-3.6, 3.6]$.

Table 7 further demonstrates the efficiency of ETI and quadratic elements for pricing American options. We find that in order to achieve an error of order 10^{-6} as obtained by the quadratic basis functions, the Crank-Nicolson, the three-level method and the linear element ETI scheme require that the mesh size be further refined at the cost of an increase in computational time.

6. Conclusion

This paper has considered the pricing of European, American and Butterfly options under two-state and three-state regime switching Merton jump diffusion model. We solved a system of PIDEs using Lagrange finite element techniques and exponential time integration methods studied in [26] and in [27]. The numerical experiments carried out in Section 5 demonstrate that the numerical schemes derived in this paper are very efficient based on the levels of accuracy achieved when compared to the performance of the existing numerical schemes for pricing options under regime-switching model with jump diffusion processes.

Indeed, our results compared with those derived in [8] and [19] achieved high rates of convergence using few quadratic basis functions. For European options under two-states and three-states of the economy, the ETI scheme solves the finite element system of equations in a single time step. For American options, the operator splitting mechanism combined with the ETI scheme produces reliable and accurate solutions within few time steps compared to the number of time steps employed in existing papers.

As an extension of the present work, the application of our technique to other types of exotic options or hybrid financial products, such as barrier options, look-back options, Asian options, game options, passport options and option-embedded insurance products, etc can be also explored. Finally, we may extend our framework to deal with different types of parameters' uncertainty.

7. Acknowledgement

The authors are very grateful to the School of Physical Sciences, University of Liverpool, United Kingdom for the financial support to carry out this research project. The authors would like to acknowledge also the gracious support of this work through the EPSRC and ESRC Centre for Doctoral Training on Quantification and Management of Risk & Uncertainty in Complex Systems & Environments (EP/L015927/1).

References

[1] S. Asmussen, F. Avram and M. R. Pistorius, Russian and American put options under exponential phase-type Lévy models, *Stochastic Processes and their Applications* 109 (1) (2004), 79–111.

[2] A.F. Bastani, Z. Ahmadi and D. Damircheli, A radial basis collocation method for pricing American options under regime-switching jump diffusions models, *Applied Numerical Mathematics* 65 (2013), 79–90

[3] F. Black and M. Scholes, The pricing of options and corporate liabilities, *Journal of Political Economy* 81 (1973), 637–654.

[4] P. Boyle and T. Draviam, Pricing exotic options under regime switching, *Insurance: Mathematics and Economics* 40 (2007), 267–282.

[5] J. Buffington and R. Elliott, American options with regime switching, *International Journal of Theoretical and Applied Finance* 5(5) (2002), 497–514.

[6] R. Cont and P. Tankov, *Financial modelling with jump processes*, 2004 Chapman & Hall/CRC.

[7] R. Cont and E. Voltchkova, A Finite difference scheme for option pricing in jump diffusion and exponential Lévy models, *SIAM, Journal of Numerical Analysis* 43(4) (2005), 1596–1626.

[8] M. Costabile, A. Leccadito, I. Massabó and E. Russo, Option pricing under regime switching jump diffusion models, *Journal of Computational and Applied Mathematics* 256 (2014), 152–167.

[9] Y. d'Halluin, P. A. Forsyth and K. R. Vetzal, Robust numerical methods for contingent claims under jump diffusion processes, *IMA Journal of Numerical Analysis* 25 (2005), 87–112.

[10] R. Elliott, L. Chan and T.K. Siu, Option pricing and Esscher transform under regime switching, *Annals of Finance* 1 (2005), 423–432.

[11] X. Guo and Q. Zhang, Closed-form solutions for perpetual American put options with regime switching, *SIAM Journal of Applied Mathematics* 64 (2004), 2034–2049.

[12] S. Ikonen and J. Toivanen, Operator splitting methods for American option pricing, *Applied Mathematics Letters* 17 (2004), 809–814.

[13] K.R. Jackson, S. Jaimungal, and V. Surkov, Option pricing with regime switching Lévy processes using Fourier space time stepping, *Proceeding of IASTED Financial Engineering and Applications (FEA 2007) September 24-26, Berkeley, CA, USA*

[14] J.D. Hamilton, A new approach to the economic analysis of non-stationary time series and the business cycle, *Econometrica* 57 (1989), 357–387.

[15] Y. Huang, P.A. Forsyth and G. Labahn, Methods for pricing American options under regime switching, *SIAM Journal on Scientific Computing* 33 (2011), 2144–2168.

[16] I. Karatzas and S.E. Shreve, *Methods of Mathematical Finance*, 1998, Springer.

[17] A. Khaliq and R. Liu, New numerical scheme for pricing American option with regime-switching, *International Journal of Theoretical and Applied Finance* 12(3) (2009), 319–340.

[18] S.G. Kou, A Jump-Diffusion Model for Option Pricing, *Management Science* 48(8) (2002), 1086–1101.

[19] Y. Lee, Financial options pricing with regime-switching jump diffusions, *Computers and Mathematics with Applications* 68 (2014), 392–404.

[20] R. Liu and J. Zhao, A lattice method for option pricing with two underlying assets in the regime-switching model, *Journal of Computational and Applied Mathematics* 250 (2013), 96–106.

[21] B. Mandelbrot, New methods in statistical economics, *Journal of Political Economy* 71 (5) (1963), 421–440.

[22] B. Mandelbrot, The variation of certain speculative prices, *The Journal of Business*, 36 (4) (1963), 394–419.

[23] R.C. Merton, Theory of rational option pricing, *Bell Journal of Economics and Management Science* 4 (1973), 141–183.

[24] C. Moler and C.V. Loan, Nineteen dubious ways to compute the exponential of a matrix, twenty-five years later, *SIAM Review* 45 (2003), 3–49.

[25] V. Naik, Option valuation and hedging strategies with jumps in volatility of asset returns, *The Journal of Finance* 48 (5) (1993), 1969-1984.

[26] N. Rambeerich, Y.D. Tangman, A. Gopaul and M. Bhuruth, Exponential time integration for fast finite element solutions of some financial engineering problems, *Journal of Computational and Applied Mathematics* 224 (2009), 668–678.

[27] N. Rambeerich, Y.D. Tangman, R. Lollchund and M. Bhuruth, High-order computational methods for option valuation under multi-factor models, *European Journal of Operational Research* 224 (2013), 219–226.

[28] A. Ramponi, Fourier transform methods for regime-switching jump-diffusions and the pricing of forward starting options, *International Journal of Theoretical and Applied Finance* 15(5) (2012), 1250037.

[29] W. Schoutens, Exotic options under Lévy models: An overview, *Journal of Computational and Applied Mathematics* 189 (2006), 526–538.

[30] G. Yin and Q. Zhang, *Continuous-time Markov chains and applications: a singular perturbation approach*, 1988, Springer.

[31] F.L. Yuen and H. Yang, Option pricing in a jump-diffusion model with regime switching, *ASTIN bulletin* 39(2) (2009), 515–539.

[32] F.L. Yuen and H. Yang, Option pricing with regime switching by trinomial tree method, *Journal of Computational and Applied Mathematics* 233 (2010), 1821–1833.

Linear				Quadratic			
M	Price	Error	Ratio	M	Price	Error	Ratio
$\Omega_x = [-3, 3], \quad \sigma_1 = 0.3$							
20	6.4942807			10	7.1651885		
40	6.8504798	3.5620(-1)		20	7.0620605	1.0313(-1)	
80	6.9887817	1.3830(-1)	2.6	40	7.0388825	2.3178(-2)	4.4
160	7.0248032	3.6022(-2)	3.8	80	7.0370445	1.8380(-3)	12.6
320	7.0338839	9.0807(-3)	4.0	160	7.0369252	1.1927(-4)	15.4
640	7.0361586	2.2747(-3)	4.0	320	7.0369177	7.5103(-6)	15.9
1280	7.0367275	5.6894(-4)	4.0	640	7.0369172	4.7305(-7)	15.9
$\Omega_x = [-2.5, 2.5], \quad \sigma_2 = 0.1$							
20	5.8318448			10	6.7068379		
40	6.1669349	3.3509(-1)		20	6.4198575	2.8698(-1)	
80	6.2776528	1.1072(-1)	3.0	40	6.3279645	9.1893(-2)	3.1
160	6.3065333	2.8880(-2)	3.8	80	6.3171558	1.0809(-2)	8.5
320	6.3138372	7.3039(-3)	4.0	160	6.3163374	8.1840(-4)	13.2
640	6.3156689	1.8316(-3)	4.0	320	6.3162836	5.3838(-5)	15.2
1280	6.3161271	4.5827(-4)	4.0	640	6.3162802	3.4031(-6)	15.8

Table 1: Numerical solutions at $K = S = 40$, for European put option under two-regime model with $\sigma_1 = 0.3$ and $\sigma_2 = 0.1$.

	Linear				Quadratic			
N	M	Price	Error	Ratio	M	Price	Error	Ratio
$\Omega_x = [-3, 3], \quad \sigma = 0.3$								
20	20	6.8621126			10	7.5126709		
40	40	7.1985901	3.3648(-1)		20	7.4030829	1.0959(-1)	
80	80	7.3339875	1.3540(-1)	2.5	40	7.3827493	2.0334(-2)	5.4
160	160	7.3696763	3.5689(-2)	3.8	80	7.38154286	1.2064(-3)	16.9
320	320	7.3785487	8.8724(-3)	4.0	160	7.3814850	5.7892(-5)	20.8
640	640	7.3807372	2.1885(-3)	4.1	320	7.3814864	1.4335(-6)	40.4
$\Omega_x = [-2.5, 2.5], \quad \sigma = 0.1$								
20	20	6.1395118			10	6.9964967		
40	40	6.4785649	3.3905(-1)		20	6.7393765	2.5712(-1)	
80	80	6.5914156	1.1285(-1)	3.0	40	6.6417966	9.7580(-2)	2.6
160	160	6.6198455	2.8430(-2)	4.0	80	6.6301192	1.1677(-2)	8.4
320	320	6.6267781	6.9326(-3)	4.1	160	6.6292841	8.3513(-4)	14.0
640	640	6.6286166	1.8386(-3)	3.8	320	6.6292392	4.4861(-5)	18.6

Table 2: Numerical solutions at $K = S = 40$, for American put option under two-regime model with $\sigma_1 = 0.3$ and $\sigma_2 = 0.1$.

Linear				Quadratic			
M	Price	Error	Ratio	M	Price	Error	Ratio
$\Omega_x = [-4.6, 4.6], \quad \lambda_1 = 0.3$							
40	9.5726396			20	10.3618709		
80	10.3330037	7.6036(-1)		40	10.5632097	2.0134(-1)	
160	10.4939141	1.6091(-1)	4.7	80	10.5469100	1.6300(-2)	12.4
320	10.5329663	3.9052(-2)	4.1	160	10.5459518	9.5822(-4)	17.0
640	10.5426681	9.7018(-3)	4.0	320	10.5459001	5.1701(-5)	18.5
1280	10.5450898	2.4218(-3)	4.0	640	10.5458970	3.1674(-6)	16.3
$\Omega_x = [-4.6, 4.6], \quad \lambda_1 = 0.5$							
40	12.1008766			20	12.9755541		
80	12.8922315	7.9135(-1)		40	13.1280912	1.5254(-1)	
160	13.0541776	1.6195(-1)	4.9	80	13.1082830	1.9808(-2)	7.7
320	13.0936244	3.9447(-2)	4.1	160	13.1067947	1.4883(-3)	13.3
640	13.1034355	9.8111(-3)	4.0	320	13.1067073	8.7366(-5)	17.0
1280	13.1058852	2.4497(-3)	4.0	640	13.1067019	5.4067(-6)	16.2
$\Omega_x = [-4.6, 4.6], \quad \lambda_3 = 0.7$							
40	13.9215882			20	14.8406817		
80	14.7035240	7.8194(-1)		40	14.9375272	9.6845(-2)	
160	14.8602701	1.5675(-1)	5.0	80	14.9137680	2.3759(-2)	4.1
320	14.8988343	3.8564(-2)	4.0	160	14.9117752	1.9928(-3)	11.9
640	14.9084483	9.6140(-3)	4.0	320	14.9116584	1.1679(-4)	17.1
1280	14.9108502	2.4019(-3)	4.0	640	14.9116512	7.1869(-6)	16.3

Table 3: Numerical solutions at $S = K = 100$, for a European put option under three regime Merton jump diffusion model.

Linear					Quadratic				
$\Omega_x = [-3.5, 3.5] \quad \lambda_1 = 0.3$									
M	N	Price	Error	Ratio	M	N	Price	Error	Ratio
16	16	6.4766039			8	16	9.0633352		
32	32	9.9791680	3.5026		16	32	11.1994005	2.1361	
64	64	10.9089120	9.2974(-1)	3.8	32	64	11.1411764	5.8224(-2)	36.7
128	128	11.0788424	1.6993(-1)	5.5	64	128	11.1261351	1.5041(-2)	3.9
256	256	11.1141262	3.5284(-2)	4.8	128	256	11.1250693	1.0658(-3)	14.1
512	512	11.1224373	8.3110(-3)	4.2	256	512	11.1250406	2.8668(-5)	37.2
$\Omega_x = [-3.5, 3.5] \quad \lambda_1 = 0.5$									
M	N	Price	Error	Ratio	M	N	Price	Error	Ratio
16	16	8.9745420			8	16	11.9917770		
32	32	12.8947292	3.9202		16	32	14.0740713	2.0823	
64	64	13.6378371	7.4311(-1)	5.3	32	64	13.8615849	2.1249(-1)	9.8
128	128	13.7876701	1.4983(-1)	5.0	64	128	13.8328230	2.8762(-2)	7.4
256	256	13.8206682	3.2998(-2)	4.5	128	256	13.8314890	1.3340(-3)	21.6
512	512	13.8287416	8.0734(-3)	4.1	256	512	13.8313990	8.9963(-5)	14.8
$\Omega_x = [-3.5, 3.5] \quad \lambda_1 = 0.7$									
M	N	Price	Error	Ratio	M	N	Price	Error	Ratio
16	16	10.8448914			8	16	14.1624739		
32	32	14.9493499	4.1045		16	32	16.1032638	1.9408	
64	64	15.5743583	6.2501(-1)	6.6	32	64	15.7933102	3.0995(-1)	6.3
128	128	15.7103160	1.3596(-1)	4.6	64	128	15.7532644	4.0046(-2)	7.7
256	256	15.7413030	3.0987(-2)	4.4	128	256	15.7516936	1.5708(-3)	25.5
512	512	15.7490041	7.7012(-3)	4.0	256	512	15.7515986	9.4970(-5)	16.5

Table 4: Numerical solutions at $S = K = 100$, for American put option under three regime Merton jump diffusion model.

Linear			Quadratic		
Regime 1: $\Omega_x = [-2,2], \sigma_1 = 0.25, r_1 = 0, \mu_1^J = 0, \sigma_1^J = 0.3, \lambda_1 = 1$					
M	Price	Error	M	Price	Error
20	1.1386893				
40	1.1028579	3.5831(-2)	20	1.0944537	
80	1.0982413	4.6166(-3)	40	1.0967580	2.3043(-3)
160	1.0971723	1.0690(-3)	80	1.0968198	6.1759(-5)
320	1.0969104	2.6190(-4)	160	1.0968234	3.6579(-6)
640	1.0968453	6.5088(-5)	320	1.0968237	2.2320(-7)
Regime 2: $\Omega_x = [-2,2], \sigma_2 = 0.2, r_2 = 0.02, \mu_2^J = -0.5, \sigma_2^J = 0.3, \lambda_2 = 0.8$					
M	Price	Error	M	Price	Error
20	0.9815562				
40	0.9355795	4.5977(-2)	20	0.9255812	
80	0.9295196	6.0599(-3)	40	0.9275855	2.0043(-3)
160	0.9280978	1.4217(-3)	80	0.9276286	4.3156(-5)
320	0.9277477	3.5012(-4)	160	0.9276313	2.7265(-6)
640	0.9276605	8.7172(-5)	320	0.9276315	1.7343(-7)
Regime 3: $\Omega_x = [-2,2], \sigma_3 = 0.15, r_3 = 0.07, \mu_3^J = 0.1, \sigma_3^J = 0.35, \lambda_3 = 1$					
M	Price	Error	M	Price	Error
20	1.2920231				
40	1.1996887	9.2334(-2)	20	1.1762833	
80	1.1881729	1.1516(-2)	40	1.1844393	8.1560(-3)
160	1.1855269	2.6460(-3)	80	1.1846507	2.1132(-4)
320	1.1848769	6.5005(-4)	160	1.1846607	1.0006(-5)
640	1.1847151	1.6175(-4)	320	1.1846613	5.7915(-7)

Table 5: Numerical solutions of a European Butterfly call option under three state economy at $K = S = 100$ and $T = 1$ year.

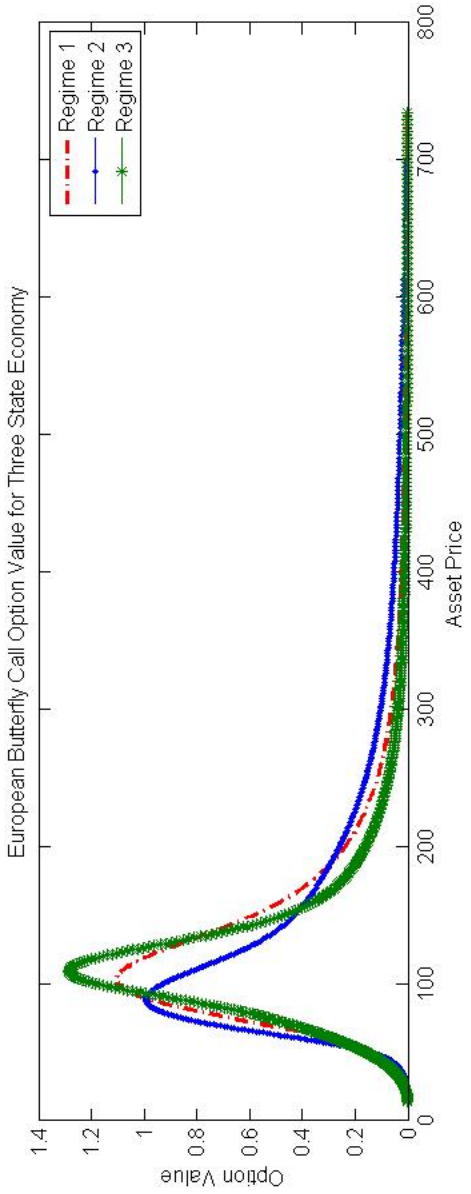

Figure 1: Illustration for a European Butterfly call option for the three state economy

Regime 1: T = 0.5, $\sigma = 0.15$, $r = 0.03$, $\delta = 0$, $\mu_1^J = 0$, $\sigma_1^J = 0.3$,$\lambda_1 = 0.3$, $\Omega_x = [-3.2, 3.2]$										
Linear Elements										
Elements	Time-Steps	$S = 90$			$S = 100$			$S = 110$		
M	N	Price	Error	CPU	Price	Error	CPU	Price	Error	CPU
40	20	9.2817579		0.1186	3.6502918		0.1186	1.1685179		0.1186
80	40	9.5824778	3.0072(-1)	0.1199	4.0620456	4.1175(-1)	0.1199	1.5238535	3.5534(-1)	0.1199
160	80	9.6767588	9.4281(-2)	0.1522	4.1495112	8.7466(-2)	0.1522	1.6058576	8.2004(-2)	0.1522
320	160	9.7008346	2.4076(-2)	0.2179	4.1706547	2.1144(-2)	0.2179	1.6265026	2.0645(-2)	0.2179
640	320	9.7069029	6.0683(-3)	0.8564	4.1759006	5.2460(-3)	0.8564	1.6316660	5.1633(-3)	0.8564
1280	640	9.7084222	1.5192(-3)	4.2615	4.1772097	1.3091(-3)	4.2615	1.6329580	1.2921(-3)	4.2615
2560	1280	9.7088022	3.8001(-4)	24.6952	4.1775368	3.2711(-4)	24.6952	1.6332810	3.2303(-4)	24.6952
5120	2560	9.7088972	9.5009(-5)	180.2659	4.1776186	8.1769(-5)	180.2659	1.6333618	8.0763(-5)	180.2659
Quadratic Elements										
Elements		$S = 90$			$S = 100$			$S = 110$		
M		Price	Error	CPU	Price	Error	CPU	Price	Error	CPU
20		9.6752514		0.1359	4.1221897		0.1359	1.4939265		0.1359
40		9.7026388	2.7387(-2)	0.1519	4.1976074	7.5418(-2)	0.1519	1.6201531	1.2623(-1)	0.1519
80		9.7084875	5.8487(-3)	0.2981	4.1786034	1.9004(-2)	0.2981	1.6326166	1.2464(-2)	0.2981
160		9.7088979	4.1035(-4)	1.4973	4.1776954	9.0804(-4)	1.4973	1.6333295	7.1290(-4)	1.4973
320		9.7089269	2.9030(-5)	13.7330	4.1776488	4.6536(-5)	13.7330	1.6333857	5.6217(-5)	13.7330
640		9.7089287	1.7815(-6)	165.2898	4.1776460	2.7985(-6)	165.2898	1.6333885	2.7932(-6)	165.2898

Table 6: European option under three regime Merton jump diffusion model: Comparison between Three Level method with linear elements and ETI with quadratic elements.

	Linear Elements						Quadratic Elements		
	Regime 1								
		Crank-Nicolson		Three-Level Method		ETI-Linear Elements		ETI-Quadratic-Elements	
N	M	Price	Error	Price	Error	Price	Error	M	Price	Error
20	40	9.5027430		7.9667815		9.5013001		20	10.4542239	
40	80	10.1260668	6.2332(-1)	10.1230743	2.1563	10.1254875	6.2419(-1)	40	10.3350667	1.1916(-1)
80	160	10.2518153	1.2575(-1)	10.2528639	1.2979(-1)	10.2515003	1.2601(-1)	80	10.2945786	4.0488(-1)
160	320	10.2810632	2.9248(-2)	10.2800591	2.7195(-2)	10.2807159	2.9216(-2)	160	10.2909149	3.6636(-3)
320	640	10.2880269	6.9637(-3)	10.2879052	7.8461(-3)	10.2879766	7.2607(-3)	320	10.2905588	3.5610(-4)
640	1280	10.2898961	1.8693(-3)	10.2898729	1.9677(-3)	10.2898793	1.9027(-3)	640	10.2905481	1.0715(-5)
	Regime 2									
N	M	Price	Error	Price	Error	Price	Error	M	Price	Error
20	40	7.6249327		7.6743089		7.6239823		20	8.2292831	
40	80	8.0275524	4.0262(-1)	8.0247599	3.5045(-1)	8.0270412	4.0306(-1)	40	8.1595185	6.9765(-2)
80	160	8.1147428	8.7190(-2)	8.1115369	8.6777(-2)	8.1141707	8.7129(-2)	80	8.1401310	1.9387(-2)
160	320	8.1336680	1.8925(-2)	8.1319106	2.0374(-2)	8.1330131	1.8842(-2)	160	8.1391892	9.4176(-4)
320	640	8.1374138	3.7458(-3)	8.1372707	5.3601(-3)	8.1373187	4.3057(-3)	320	8.1391006	8.8622(-5)
640	1280	8.1386386	1.2248(-3)	8.1386356	1.36489(-3)	8.13863407	1.3153(-3)	640	8.1390950	5.5961(-6)
	Regime 3									
N	M	Price	Error	Price	Error	Price	Error	M	Price	Error
20	40	7.6091107		7.6354691		7.6083123		20	8.2978275	
40	80	8.0909106	4.8180(-1)	8.0924661	4.5700(-1)	8.0906044	4.8229(-1)	40	8.2519941	4.5833(-2)
80	160	8.1904002	9.9490(-2)	8.1881347	9.5669(-2)	8.1901715	9.9567(-2)	80	8.2220602	2.9934(-2)
160	320	8.2130304	2.2630(-2)	8.2118561	2.3721(-2)	8.2127800	2.2608(-2)	160	8.2199214	2.1388(-3)
320	640	8.2180783	5.0479(-3)	8.2178108	5.9546(-3)	8.2179385	5.1586(-3)	320	8.2197802	1.4112(-4)
640	1280	8.2192803	1.2021(-3)	8.2192797	1.4690(-3)	8.2192771	1.3386(-3)	640	8.2197719	8.3545(-6)

Table 7: Numerical solutions for American put option under three state economy computed at $K = S = 100$.